Experimental validation and uncertainty analysis of an innovative IoT infrared sensor for in-situ wall thermal transmittance measurement

Experimental validation and uncertainty analysis of an innovative IoT infrared sensor for in-situ wall thermal transmittance measurement

Serena Serroni[1*], Marco Arnesano[2], Milena Martarelli[1], Gian Marco Revel[1]

[1] Università Politecnica delle Marche, Department of Industrial Engineering and Mathematical Science, Via delle Brecce Bianche, 60131 Ancona (AN), Italy
[2] Università Telematica eCampus, Via Isimbardi 10,22060 Novedrate (CO), Italy

* Corresponding Author: s.serroni@pm.univpm.it

Abstract

This paper presents the development and experimental validation of an Internet of Things (IoT) thermography system for in-situ and real-time monitoring of wall thermal transmittance. The solution proposed has been derived from the upgrade of the Comfort Eye sensor, which is an infrared-based sensor adopted for non-intrusive indoor environmental quality monitoring in occupied buildings. In this work, the system has been used to detect potential building envelope inefficiencies and track building performance trends in a continuous way. The methodology is based on the ISO 9869-2 standard but it has been applied to an entire wall and during its normal functioning without the need of operators. The data management has been performed with a dedicated IoT architecture that allows the synchronised collection of quantities required for transmittance calculation, i.e. indoor and outdoor air temperatures together with the thermographic maps of the wall. The measurement technique has been validated in a real building through the comparison with the results obtained using a heat flux meter (HFM). An uncertainty analysis with Monte Carlo simulation has also been performed to evaluate the overall uncertainty of the method. The values obtained are coherent with those measured with the HFM and the IR system has proved to be able to provide thermal transmittance measurements with an expanded uncertainty of ±0.038 W/m^2K with coverage factor k=2. The innovative methodology described can be used for U-value estimation without the need for extra measuring tools.

Keywords: IoT Infrared sensor, thermal transmittance, Monte Carlo simulation, energy efficiency, building envelope.

Nomenclature

ASHRAE American Society of Heating, Refrigerating and Air-Conditioning Engineers

AVGM Average Method

BIM Building Information Model

$c(x_i)$ *Sensitivity Coefficient of the* x_j *input estimate*

cdf cumulative density function

ε *Emissivity*

GUM Guide to the expression of Uncertainty in Measurement

h *Heat transfer coefficient*

h_c *Convective heat transfer coefficient*

HF Heat Flux

HFM Heat Flux Meter

h_r *Radiative heat transfer coefficient*

IEQ Indoor Environmental Quality

IoT Internet of Things

IRT Infrared Thermography

IR Infrared

L *Component thickness*

M *Number of trials*

MCM Monte Carlo Method

pdf probability density function

PM Particulate Matter

q *heat flux*

Q_{cond} *Conductive heat flux*

Q_{conv} *Convective heat flux*

Q_{rad} *Radiative heat flux*

RH Relative Humidity

ROI Region Of Interest

σ *Stefan*-Boltzmann constant

S_i *Sensitivity index with respect to the* x_i *input estimate*

T_a *Air temperature*

T_{atm} *Atmosphere temperature*

T_e Outdoor air temperature

T_i Indoor air temperature

T_{refl} Reflected temperature

T_{si} Indoor surface temperature

T_{tot} Total temperature

$u(x_i)$ Standard uncertainty associated with the input estimate x_i

$u(y)$ Uncertainty of the output y

V_{xi} Variance due to the perturbation of the model associated with the input estimate x_i

V_{tot} Total variance of the output due to the perturbation of the model

1. Introduction

Buildings are one of the major contributors to global energy consumption, therefore improving building energy efficiency has become a strategic and crucial issue. In [1] and [2] it was reported that roughly 40% of global energy is consumed by buildings. Particularly in [1] the authors pointed out that the difficulty in reducing this percentage lies in the gap between the energy performance predicted in the project phase and the actual energy performance measured [3]. Over the last years, various approaches have been used to monitor and improve building energy performance. In [4], for example, the authors proposed the long-term observation of electric parameters combined with methods and algorithms that can evaluate buildings' ageing process and an intelligent control that further enables local energy management on the part of consumers as well as consumption management in smart grids. In [2] measurement and control were extended also to health and comfort monitoring for a smart building concept. Whereas in [5] a machine learning approach was presented with the purpose of predicting the energy performance (heating load and cooling load) of residential structures.

One of the most critical elements affecting the heating and cooling energy consumption in built environments is the thermal performance of their envelopes [6][7]. When the stratigraphy of the envelope component is known, the thermal transmittance (U-value) can be determined using the EN ISO 6946 standard [8] with an uncertainty range of 5–50%, or it can be calculated using laboratory testing in line with the EN ISO 8990 standard [9]. Both the methods have the limitation that, when building elements are unknown, for the implementation of the standards, core boring or endoscopic tests, which are destructive, or alternatively laboratory tests, which are not always feasible, are required.

The ISO 9869-1 standard [10] defines a method for in-situ thermal transmittance measurements which makes use of contact sensors, e.g., thermocouples and HFMs (Heat Flux Methods). However, these are a local measurement which are often not indicative of the dynamic thermal response of a whole wall, particularly in prefabricated panels with a complex internal structure. In-situ measurements are also affected by environmental conditions [11], which, however, can be statistically cancelled out if the measurement duration is longer than the typical daily environmental cycle, which is the reason why the standard requires a test to last at least 72 hours. The thermal conductivity measured using an HFM is also affected by radiative heat losses, as evidenced in [12]. This interfering input cannot be neglected if the heat flow is not purely mono-directional. To make sure that this hypothesis is verified, the mounting position of the HFM needs to be identified a priori.

In [13] the authors described an alternative to the method defined in ISO 9869-1 which has two upgrades:

- an additional HFM on the external surface of the building façade, besides the sensor installed on the interior side as suggested by the standard;
- the calculation of thermal transmittance from the heat flux obtained from the average of the heat fluxes measured by the two sensors.

These methods allow a reduction of both measurement time (from the minimum required 72 hours down to 24 hours) and uncertainty of the thermal transmittance measurement (from 8% to 5%).

Nevertheless, environmental conditions remain an interfering input when assessing thermal transmittance. To reduce their influence on heat flow and temperature measurements, in [11] the authors proposed to apply an artificial thermal load produced by a heating box to the façade wall where the sensors are mounted. On the one hand, the approach reaches an accuracy of 4.4–7.5%. On the other hand, however, the procedure is extremely time consuming. A hybrid method to improve the robustness of U-value estimation of building envelopes was proposed in [14]. The method integrated the experimental data measured by means of heat flux sensors with the U-value calculation of wall surface via a mono-dimensional nodalisation of the wall itself. Numerical and experimental data were exploited in an optimisation problem based on the minimisation of the RMS values of the deviations of both the calculated and experimental heat fluxes. This method can be applied to any kind of wall, including those with a complex stratigraphy, since it makes it possible to assess an equivalent conductivity and calculate wall conductance and its equivalent thermal capacity.

All the methods described above make use of contact sensors (thermocouples and heat flow meters), which limit the evaluation of thermal transmittance to punctual values in the space. As a consequence, due to the difficulty in accounting for the potential existence of thermal bridges in the test wall, the U-value computed is underestimated. Due to this, the use of infrared sensors for measuring the U-value has recently been investigated, for example in [15]. In fact, thermal cameras, which make use of IR sensors, make it possible to frame large portions of building envelopes and identify regions with unusual thermal behaviour (such as local thermal bridges, regions with excessive moisture content), which can be and excluded from further research. The primary drawback of this approach is that it has a poor repeatability index for light walls and super-insulated constructions because IR sensors are highly dependent on ambient factors (external radiation, wind), which results in low accuracy values with an uncertainty of up to 20% [16]. Some studies suggested using thermal cameras to estimate thermal transmittance when the test wall is under quasi steady-state ([17], [18]) or steady-state ([19]) conditions by detecting heat flow and surface temperature. However, this kind of conditions are impractical and can very rarely be reproduced in real environments. Other works overcame this difficulty by considerably increasing test durations to reduce the error related to the variability of environmental conditions ([20], [21], [22]).

The ISO 9869-2-2018 standard regulates the use of thermography for the estimation of the U-value in built environments [23]. The standard also introduces a method to calculate the heat transfer coefficient (h) in-situ, which is considered critical in real settings. The methods used to calculate h are the IR camera and the active heat flux meter. To estimate thermal transmittance, the standard advises taking measurements at night for a minimum of three consecutive days. Alternatively, measurements may end once thermal transmittance, computed using the moving average technique, converges to a constant value with a variance of less than 10%.

The system and approach proposed in this study are based on the estimation of the U-value of a building element which is derived from the indoor surface temperature obtained using an IoT system, Comfort Eye [24][25]. This study intends to investigate and delve further into Comfort Eye's functionality, which typically makes it possible to measure the data required for Indoor Environmental Quality (IEQ). The Comfort Eye sensor consists of two nodes, i.e. a ceiling node with an infrared sensor and a desk node with sensors for the measurement of environmental parameters. When in a scanning mode, the IR sensor can frame the whole walls of the room where it is installed. In the case of façade walls, it enables the continuous monitoring of the thermal dynamic behaviour of the walls. The approach, which was developed within the European project BIMSPEED [26], is based on the estimation of the heat flow from the indoor surface temperature obtained using the ceiling node and was tested in a real setting using an HFM as a reference. The system was installed in the laboratory at the Polytechnic University of Marche in January 2022. An uncertainty analysis based on Monte Carlo simulations was also performed to analyse the overall uncertainty of the method as well as the impact of the uncertainty of the input variables on the U-value measurement output [27].

2. Methodology

2.1 Transmittance calculation

IR thermography makes it possible to assess the surface temperature of an object by measuring the distribution of the radiant thermal energy (radiant heat transfer) emitted by the hot surface. If the object is a building element like a façade wall experiencing a thermal gradient between its internal and external surface, the surface temperature can be related to the thermal properties of the wall and specifically to its thermal transmittance. To analytically quantify this relation, an understanding of the different types of heat transfer arising between the surface of the building element and the IR sensor is required [28]. A generic component of thickness L (in m) as sketched in Figure 1 is considered and exposed to a thermal load (on the right of the sketch) that induces a surrounding air temperature of $T_{i,load}$ and a wall surface temperature of $T_{si,load}$. If the temperatures of the air and wall surface on the left of the sketch are different, due to the thermal gradient, the component experiences a conductive heat flux through the material (Q_{cond}) which depends on the transmittance properties of the material itself. The temperature of the wall surface on the left of the sketch ($T_{si,mean}$) depends on the conductive heat transfer and it is measured by the IR camera sensor, which is also sensitive to the radiant and convective flows (Q_{rad} and Q_{cond}) between the wall and the sensor itself [29].

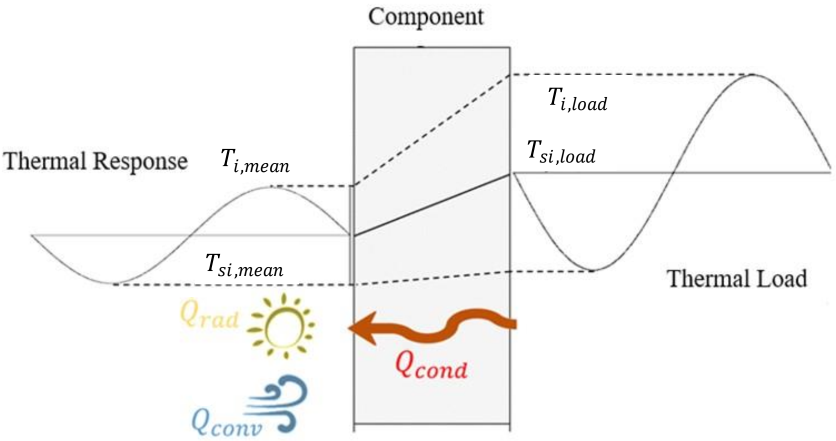

Figure 1 Thermal dynamic behaviour of a building component (wall)

The equilibrium condition between the building component and its surrounding air is obtained when the conductive heat flux is equal to the sum of the radiative and convective heat fluxes, as expressed in Equation (1):

$$Q_{cond} = Q_{conv} + Q_{rad} \tag{1}$$

where Q_{cond} is the conductive heat flux and Q_{conv}, and Q_{rad} are the convective and radiative fluxes, respectively (W/m^2). With regards to the convective heat flux states:

$$Q_{conv} = h_c \times (T_i - T_{si}) \tag{2}$$

where h_c is the convective heat transfer coefficient (W/(m^{2}K)), T_i the indoor air temperature (K), and T_{si} the surface temperature (K). With regards to the radiative heat flux states:

$$Q_{rad} = h_r \times (T_i - T_{si}) \tag{3}$$

where h_r is the radiative heat transfer coefficient (W/(m^{2}K)).

According to Acikgoz et al. [30], h_r , which is calculated using Equation (4), has a constant value at low temperatures (-10°C to 50°C):

$$h_r = \varepsilon \times \sigma \times (T_i^4 - T_{si}^4)/(T_i - T_{si}) \tag{4}$$

where σ is the Stefan-Boltzmann constant (5.67 * 10 $^{-8}$ W/m^{2}K^4) and ε is the emissivity of the wall surface.

The coefficient h_c can be calculated using analytical, numerical, or experimental approaches. The latter are the primary way for calculating h_c. However, empirical equations are influenced by a wide variety of conditions. With regards to natural convection, h_c can be expressed using Equation (5) for every surface [31][32].

$$h_c = \mathrm{C} \times \Delta T^n \tag{5}$$

where *C* and *n* are constants and can be found in literature, and $\Delta T = T_i - T_{si}$. Different authors provide different values which are listed in , respectively.

Table 1.

For vertical surfaces, in ISO 6946 [8] and ISO 9869 [10] h_c is supposed to be 2.5 W/m^{2}K and 3.00 W/m^{2}K, respectively.

Table 1 Values of C and n defined by different authors and used to calculate the h_c coefficient [32]

Authors	$\boldsymbol{h_c}$**(W/(m^{2}K))**
Khalifa et al.	$2.07 \times \Delta T^{0.230}$
Awbi et al.	$1.49 \times \Delta T^{0.345}$
Michejev	$1.55 \times \Delta T^{0.330}$
King	$1.51 \times \Delta T^{0.330}$
Nusselt	$2.56 \times \Delta T^{0.250}$
Heilman	$1.67 \times \Delta T^{0.250}$
Wilkers et al	$3.04 \times \Delta T^{0.120}$
ASHRAE	$1.31 \times \Delta T^{0.330}$
ISO 9869	3.00
ISO 6946	2.5

The IR sensor provides the T_{si} measurement, and therefore it makes it possible to estimate the radiant and convective fluxes (by Equation (2) and (3)). Hence, the U-value is calculated with the moving average method (AVGM) according to Equation (6):

$$\mathrm{U} = \sum_{j=1}^{N} (Q_{rad} + Q_{conv}) \Big/ \sum_{j=1}^{N} (T_i - T_e)_j \tag{6}$$

where T_e is the outdoor air temperature, T_i is the indoor air temperature, and the index j counts the running measures considered in the moving average process. T_i is provided by Comfort Eye's desk node, and T_e is measured by a weather station. The reference U-value from the HFM measurement is calculated using the following equation:

$$U = \sum_{j=1}^{N} q_j \,/\, \sum_{j=1}^{n} (T_i - T_e)_j \tag{7}$$

where q_j is the heat flux and T_i , T_e are the indoor and outdoor air temperature, respectively, while index j counts the individual samples.

To consider the small variability of the quantities measured, the final U-value is calculated as the mean of the last 10 samples for both models, i.e. the HFM model and the IR model.

2.2 Comfort Eye: IR sensor

Comfort Eye [33] is an IoT and low-cost system which makes it possible to assess the thermal dynamic behaviour of a whole wall through the real-time and continuous thermal monitoring of the building. The sensor consists of 2 nodes, i.e., a ceiling node with an infrared sensor, and a desk node that measures relative humidity (*RH*), CO_2, indoor air temperature (T_i), and Particulate Matter (*PM*) using two sensors, namely Sensirion SPS30, which measures PM, and Sensirion SCD30, which measures T_i, *RH*, and CO_2 in a single point. The ceiling node that detects the wall's inside surface temperature (T_{si}) is Comfort Eye's key innovative aspect. It is a 2-axes rotating 3D thermal scanner (MLX90621) that produces thermal maps of interior surface temperatures. The IR system consists of a 16x4 thermopile array; thus, each frame captured has a map of 64 wall temperatures and a field of view of 60x16°. Therefore, at the distance of one meter from the sensor, the area scanned is of 1.15 x 0.56 m. The device entails a custom mainboard with a microcontroller, programmed with dedicated firmware, to perform the automatic scanning of all the room's surfaces by controlling the horizontal and vertical movements of servos. All the specifications of the sensors are given in **Errore. L'origine riferimento non è stata trovata.**.

Table 2 Specifications of Comfort Eye's sensors (Ceiling node and Desk node)

Sensors	Range	Accuracy	Repeatability
IR sensor	-20 °C – 300 °C	± 1 °C	/
CO_2	0-40000 ppm	± (30ppm + 3%MV)	±10 ppm
RH	0%-100%	±3%RH	±0.1%RH
$\boldsymbol{T_i}$	-40 °C-70°C	± (0.4 + 0.023 ×(T[°C]-25°C))	±0.1°C
PM2.5	0-1000(μg/m^3)	±10 (μg/m^3)	/

PM10	0-1000($\mu g/m^3$)	±10($\mu g/m^3$)	/

In Figure 2, the IoT architecture of the entire system is illustrated.

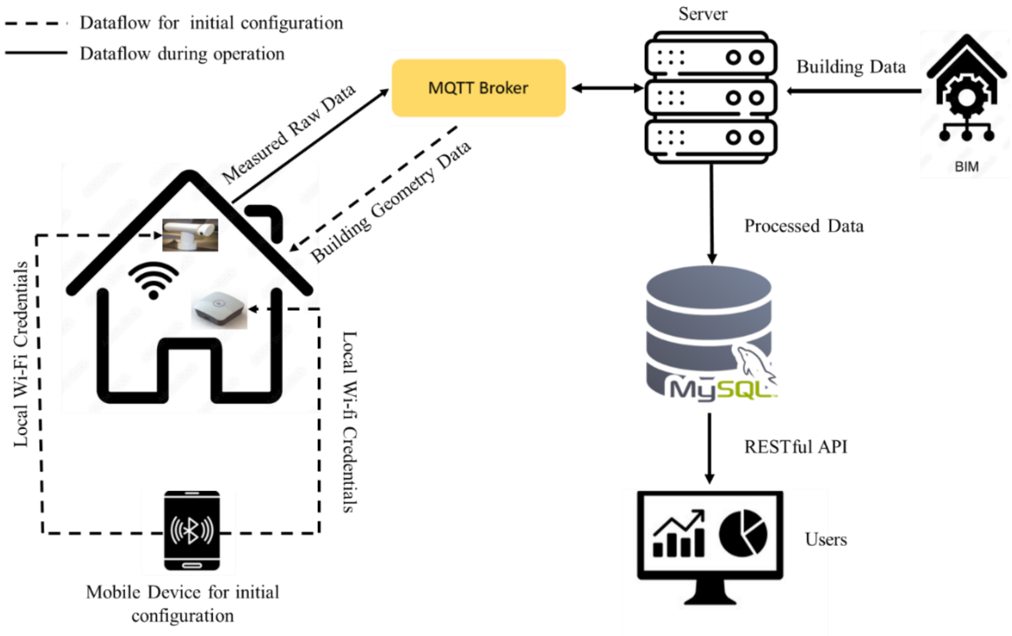

Figure 2 Comfort Eye's general architecture. The system is composed of a ceiling node with an infrared sensor that scans the whole walls of the room and a desk node that acquires environmental parameters. The configuration and operation dataflows are managed by means of a dedicated architecture that integrates mobile devices and a remote server for data processing.

Once the two nodes are installed in the building to be tested, the Wi-Fi network credentials are sent via Bluetooth, the nodes then connect to the local network, and the data are sent to the server, processed, and stored in a MySQL database. The entire process is real-time and continuous. The communication module used is the PyCOM W01, which implements Bluetooth Low Energy and supports the Message Queuing Telemetry Transport (MQTT) protocol. A dashboard was developed for the evaluation of thermal performance and data exploration. The dashboard is a web app that is accessible via any browser. Core data processing is served by a RESTful API (Application Programming Interface) running on the server and retrieved with a standard GET request.

The thermographic images are corrected taking into account the wall geometry, which, if available, can be automatically extracted from the Building Information Model (BIM), the reflected temperature and the emissivity of the wall. A detailed description of the IR scan sensor can be found in [33], while in [34] a thorough description of the IoT architecture of the system is provided.

3. Experimental test setup

The methodology presented was validated in a real environment using an HFM as a reference. The system was installed in a room of the laboratory at the Polytechnic University of Marche in January 2022. The wall analysed has a thickness of 0.40 cm and is composed of three layers, i.e. a concrete layer of 0.15 cm, an insulation layer of 0.10 cm, and a second concrete layer of 0.l5 cm.

The sensors were configured to collect data every four minutes. The measuring campaign was conducted in the period between 2nd February 2022 and 3rd March 2022 on a wall with windows that were not directly exposed to solar radiation. The exterior surface of the wall overlooks onto an atrium and is shielded from weather conditions by the atrium's roof. In the period considered, the inside environment was heated by radiators from 7:00 a.m. until 9:00 p.m. The measurements were carried out in accordance with ISO 9869-1 [10] for the HFM method and ISO 9869-2 [23] for the IR method. In particular, for the HFM measurements the following protocol was considered:

- the heat flux sensor was not positioned in proximity to the components with high thermal conductivity;
- the surface examined was shielded from weather conditions (rain, wind, solar radiation);
- the time intervals between data acquisitions were less than 30 minutes;
- the measuring time for stable boundary temperatures exceeded 72 hours.

As far as the IR method is concerned, in accordance with ISO 9869-2, the experimental data were considered valid only when the difference between indoor and outdoor air temperatures was at least 10° C. The IR scanning system (Comfort Eye) was installed in front of the wall under test with the two fixed rotary axes to measure the superficial temperature of the wall. Comfort Eye's desk node, which was used to measure the internal temperature, was placed in an environment-representative location away from heat sources, sunlight, direct ventilation, and other factors that could interfere with the measurements. As a reference system, six Type T thermocouples were mounted on the internal surface of the wall, so as to monitor the surface temperatures. In addition, a thermocouple was placed inside the room and a further one outside the room, so as to measure the room's outdoor and indoor air temperatures. Two heat flux transducers (HFP01 sensor based on thermopile [35]) were mounted on the internal surface of the wall to monitor the thermal flow through its thickness. A thermocouple was mounted on a piece of low-emissivity aluminium foil placed on the surface scanned by the infrared camera to measure the reflected temperature and correct the measured temperature from the energy reflected by the environment. The emissivity of the wall was calculated using the reference method, i.e. by installing a 3M insulating tape with known emissivity of 0.95 on the wall. The U-value was calculated in the same Region of Interest (ROI) of the HFM (Figure 3), therefore considering only the values relating to the wall without the thermal bridge.

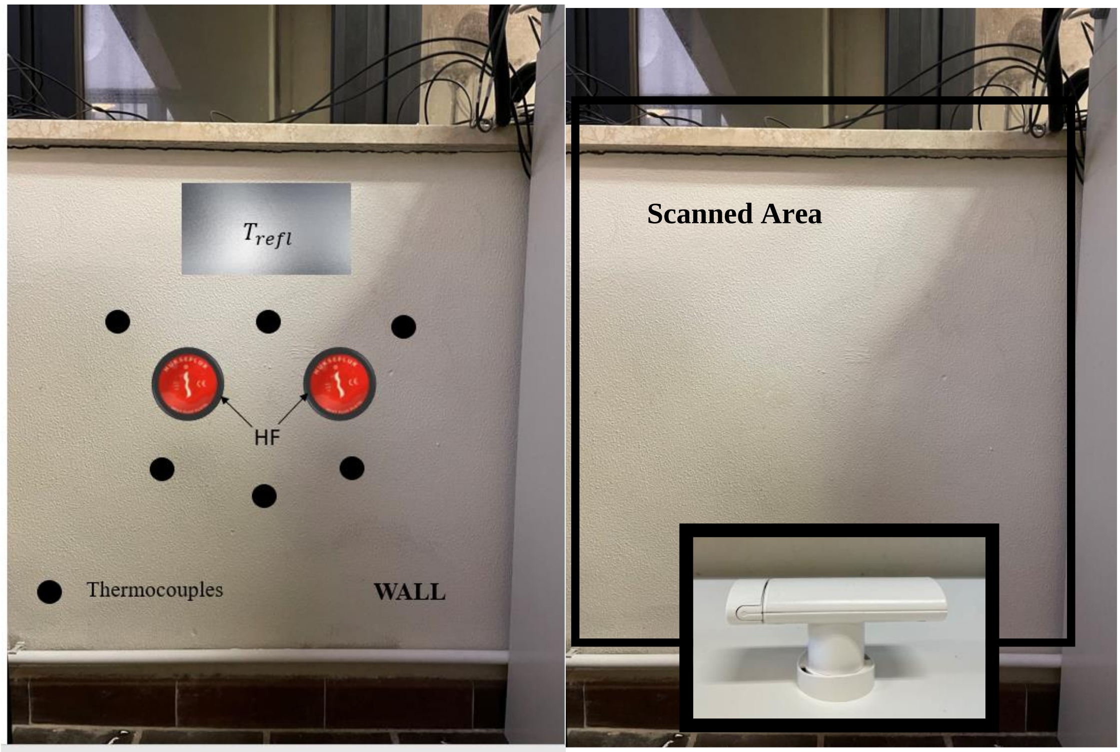

Figure 3 Experimental setup. The figure on the left shows the wall analysed using the reference system (heat flow meter and thermocouples) and the aluminium foil to measure the reflected temperature. The figure on the right shows the wall analysed using Comfort Eye

The temperature of the wall surface (T_{si}) scanned by Comfort Eye's IR sensor was corrected by applying Equation (8):

$$T_{si}^4 = \frac{1}{\varepsilon\tau} T_{tot}^4 - \frac{1-\varepsilon}{\varepsilon} T_{refl}^4 - \frac{1-\tau}{\varepsilon\tau} T_{atm}^4 \tag{8}$$

where τ is the constant atmospheric transmission coefficient, which is assumed to be equal to 0.99, ε the emissivity of the surface being measured, T_{refl} the reflected temperature computed by measuring the contribution of the opposite surface with an ε set equal to 1, T_{tot} the raw value of the total temperature detected by the IR sensor of the ceiling node, and T_{atm} the temperature of the atmosphere, which is considered to be equal to indoor air temperature (T_i).

The correction equation is necessary because the raw values detected by the IR sensor can be affected by various factors, such as the emissivity and reflectivity of the surface being measured, as well as the temperature of the atmosphere. By applying this equation in the pre-processing phase, it was possible to obtain a more accurate temperature reading of the wall surface, which is important in studies related to thermal transmission calculation.

Figure 4 shows a thermogram acquired during the test performed to measure the ε of the wall using InfraTec-Head 980. The emissivity obtained was 0. 95.

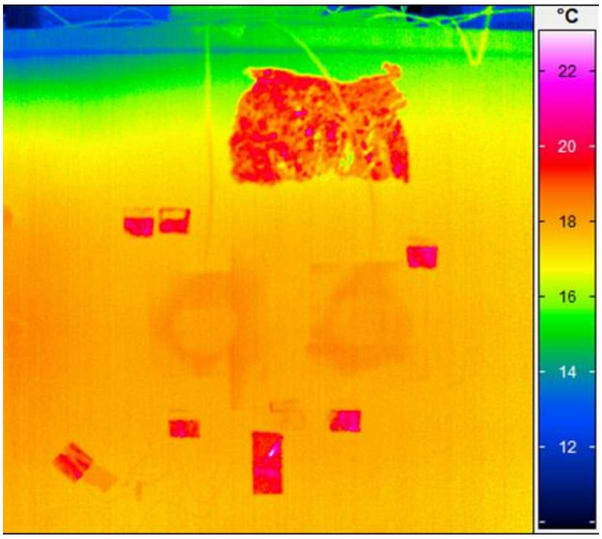

Figure 4 Thermogram of the wall acquired using the InfraTec Head 980 IR camera for the estimation of wall emissivity

4. Results

The outcomes of the tests conducted are reported in Figures 5-6-7, which compare the thermal transmittance calculated using both the methodologies, i.e. the HFM and Comfort Eye with the U-values calculated using the h_c coefficient given by ASHRAE (American Society of Heating, Refrigerating and Air-Conditioning Engineers) in three different time windows (I, II, III). The analysis was initially performed considering the h_c values given by the different authors (Table 1). In previous work [24] the authors showed that optimal results are obtained when using the value of h_c defined by Wilkers. However, under the conditions of the study here presented, the analysis demonstrated that the h_c coefficient given by ASHRAE makes it possible to obtain the best results. The uncertainty analysis discussed in the next section confirms the selection of the model based on the h_c coefficient calculated by ASHRAE.

In details, Figure 5Figure 6Figure 7 show (a) the trend of the indoor surface temperature T_{si} measured using Comfort Eye's IR sensor and a Type T thermocouple, and (b) the external temperature T_e measured with the Type T thermocouple used to calculate the thermal transmittance in the period considered. The figures also show (c) the trend of the heat flux calculated using Comfort Eye and the HFM together with the corresponding temperature difference $\Delta T = T_i - T_e$, and (d) the trend of the U-value estimated with both Comfort Eye and the reference method based on HFM. Three different 120 h time windows are reported in the three figures to demonstrate the repeatability of the model applied. According to ISO 9869-2, the difference between indoor and outdoor air temperature ΔT must be greater than 10 °C for at least 50 % of the time window considered.

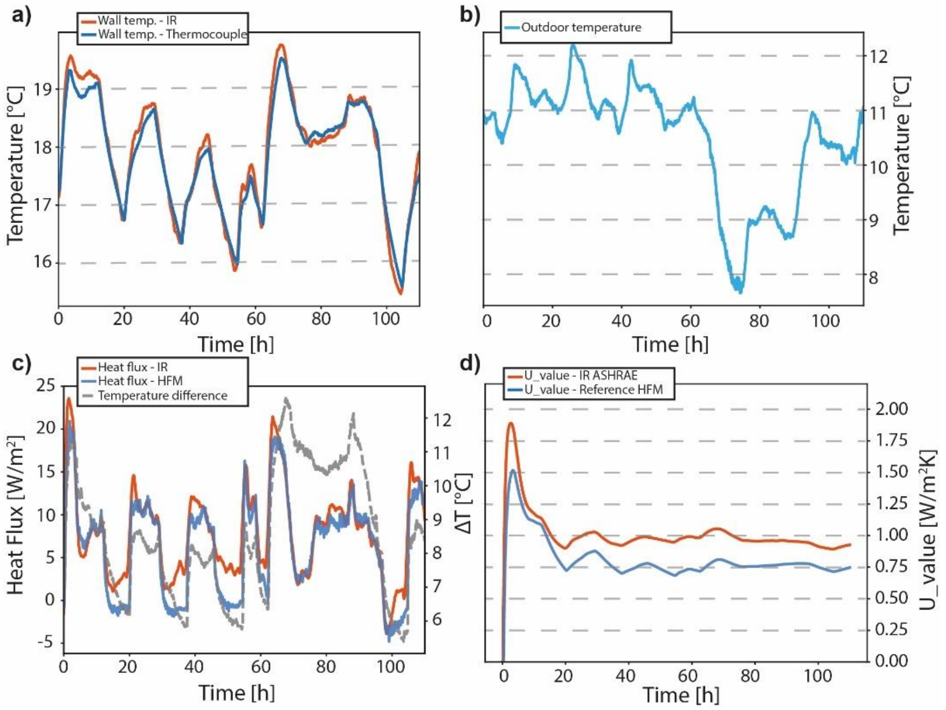

Figure 5 Time window I - trends: a) indoor wall temperature measured using the IR sensor (Comfort Eye) and the reference thermocouple, b) external temperature, c) heat flux obtained using the IR sensor (Comfort Eye) and the HFM with the corresponding ΔT, d) U-value estimated using the IR sensor (Comfort Eye) and the HFM

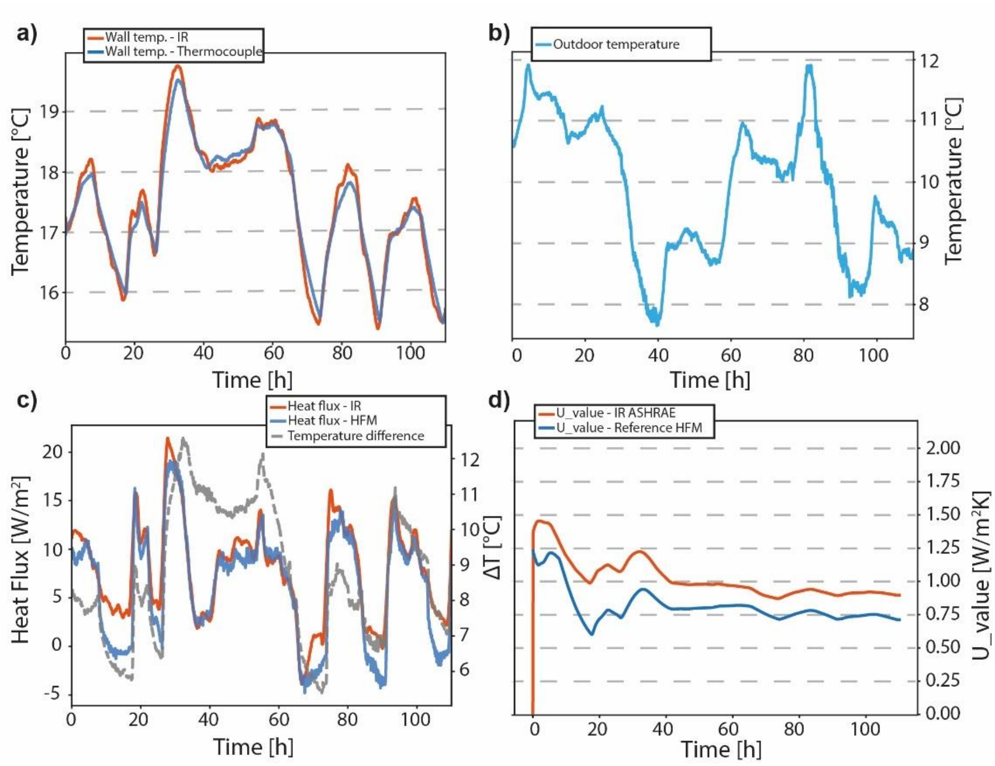

Figure 6 Time window II - trends: a) indoor wall temperature measured using the IR sensor (Comfort Eye) and the reference thermocouple, b) external temperature, c) heat flux obtained using the IR sensor (Comfort Eye) and the HFM with the corresponding ΔT, d) U-value estimated using the IR sensor (Comfort Eye) and the HFM

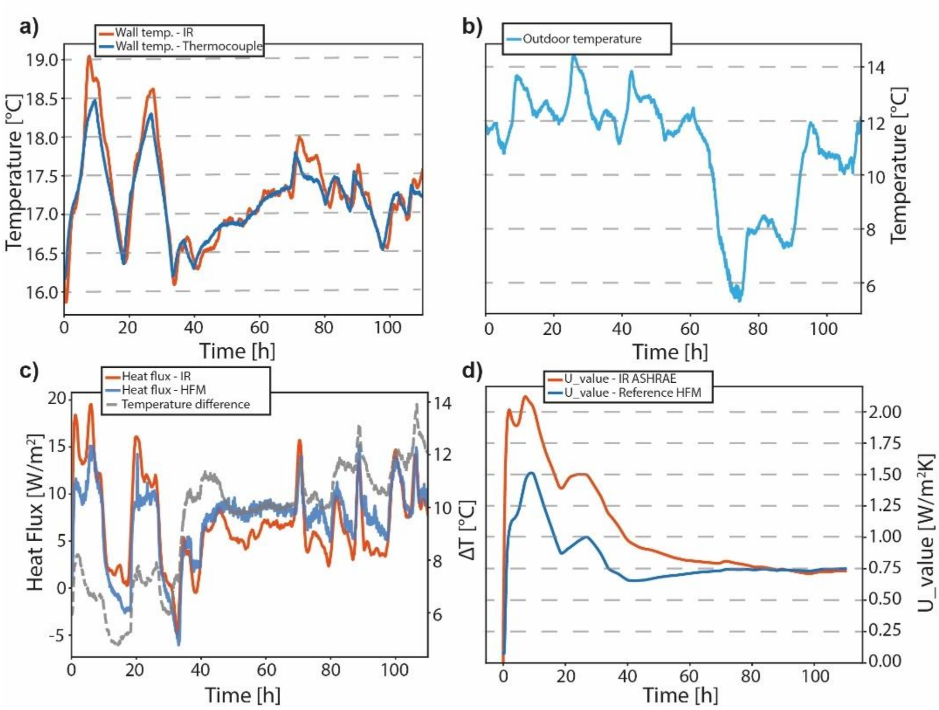

Figure 7 Time window III - trends: a) indoor wall temperature measured using the IR sensor (Comfort Eye) and the reference thermocouple, b) external temperature, c) heat flux obtained using the IR sensor (Comfort Eye) and the HFM with the corresponding ΔT , d) U-value estimated using the IR sensor (Comfort Eye) and the HFM

Considering the different time windows, the result obtained in time window I (Figure 5) is a U-value of 0.92 W/m^{2}K against the U-value of 0.74 W/m^{2}K measured using the HFM. In time window II (Figure 6) the result is a U-value of 0.89 W/m^{2}K against the U-value of 0.71 W/m^{2}K measured using the HFM, while in time window III (Figure 7) the result is a U-value of 0.73 W/m^{2}K against the U-value of 0.75 W/m^{2}K estimated with the HFM.

5. Measurement Model

The primary objective of this study is to develop a cutting-edge mathematical model for measuring thermal transmittance (U-value) using an innovative IoT system called Comfort Eye. This system enables continuous and real-time monitoring, surpassing the limitations of conventional methods. The Comfort Eye system comprises two nodes: a rotating two-axis infrared (IR) sensor typically installed at the ceiling's center to scan all walls of the room, in this study, the IR node is positioned with fixed rotating axes at 1-meter distance from the wall under analysis, the area scanned is of 1.15 x 0.56 m, and a desk node for measuring environmental parameters. The desk node is strategically positioned away from heat sources and direct solar radiation. The IR sensor captures surface temperature data T_{si}, critical for U-value calculation, and the desk node records indoor temperature T_i, another essential input for the model. External temperature can be measured by a thermocouple or extracted from an external weather station via an API service T_e. The emissivity of the wall (ε) is determined using InfraTec-Head 980 and a reference method involving the installation of a 3M insulating tape with a known emissivity of 0.95 . The sensors were configured to collect data every four minutes. The measuring campaign was conducted in the period between 2nd February 2022 and 3rd March 2022 in order to satisfy the requirements defined by ISO 9869-1 [10] and ISO 9869-2. The mathematical model employs various input variables, including corrected surface temperature T_{si}, indoor temperature T_i, external temperature T_e, and emissivity ε, to calculate the U-value.

Mathematical Model:

The Comfort Eye mathematical model is derived from equations 2 to 6, which consider the essential input variables for U-value calculation. The corrected surface temperature is obtained through meticulous processing, considering factors like emissivity and geometry (Equation 8). The desk node records continuous indoor temperature readings, while the external temperature is measured by the thermocouple or obtained from an external weather station. The emissivity of the wall is determined using a reliable reference method. With these variables and relevant constants (σ, C, n), equations 4 and 5 yield h_r and h_c. Equations 2 and 3 are then applied to determine heat flux (Q_{cond} and Q_{rad} , respectively). The final U-value is calculated using equation 6, incorporating Q_{cond}, Q_{rad}, and indoor and outdoor temperatures ($T_{i.}T_e$)

Uncertainty Analysis:

To evaluate measurement uncertainty, the Monte Carlo Method (MCM) is employed. The MCM approach generates uncertainty distributions for each input variable without direct mathematical model ($T_{si}, T_i, T_e, \varepsilon$), considering standard deviations obtained from datasheets or previous studies. Through this simulation, the uncertainty in U-value measurements is determined, aiding in understanding the measurement accuracy of the model under real environmental conditions. The results demonstrate the influence of different variables on measurement uncertainties, with temperature-related variables playing a significant role.

6. Uncertainty estimation and sensitivity analysis

6.1 Monte Carlo analysis

In this study, a method for the evaluation of the effect of the uncertainty related to input variables on U-value calculation is applied. When reporting the result of the measurement of a physical quantity, it is mandatory to provide a quantitative indication of the quality of the result, so that its reliability can be assessed. The Guide to the Expression of Uncertainty in Measurement (GUM) [27] defines the uncertainty assessment of a numerical model by using a Monte Carlo Method (MCM) [37](Figure 8).

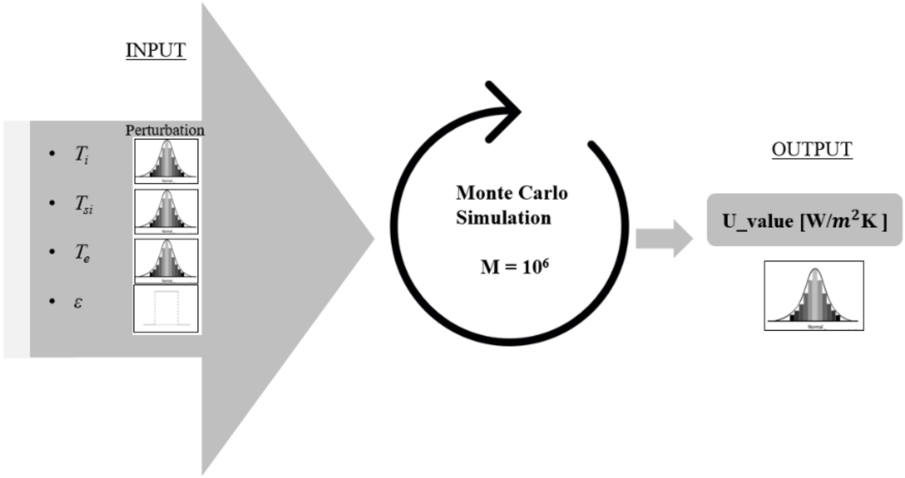

Figure 8 Input variables (T_{si} , T_i , T_e , ε) for the MCM

This approach is based on the generation of uncertainty distributions of data associated to each input of the model, to have a statistical distribution of the variables from which the uncertainty of the model can be evaluated in terms of standard deviation. For each measured data used as input of the model, the uncertainty of the specific sensor was considered and a Monte Carlo simulation was performed by generating random numbers in these uncertainty ranges by assuming a uniform or Gaussian distribution. The uncertainty of the model in terms of standard deviation was calculated by perturbing all the input variables simultaneously. In the study here presented, the sensitivity coefficients were calculated according to Annex B of JCGM 101:2008 by perturbing the value of each input parameter while keeping all the other parameters constant and then propagating the uncertainty through the model to calculate the resulting uncertainty in the output.

The conceptual description of the uncertainty estimation via the Monte Carlo method and the sensitivity analysis for the thermal transmittance measurement model are summed up in Figure 9. It consists of inputs directly measured by different sensors and a mathematical model based on the equations from (2) to (6) presented in Section 2.1. The inputs are:

1. the surface temperature T_{si}, measured by the ceiling node of the comfort eye,
2. the indoor temperature T_i, measured by the desk node of the comfort eye,
3. the external temperature T_e, measured by a thermocouple applied to the wall external surface or retrieved from nearby weather stations
4. the emissivity of the wall (ε) which must be known or measured on purpose.

The Monte Carlo method has been employed for propagating uncertainties of variables that cannot be explicitly modelled using mathematical equations. When calculating the thermal transmittance (U-value), the only variables without a direct mathematical model are T_i , T_{si}, T_e, ε . Additionally, Figure 9 enhance the clarity of the measurement model and define the interrelations among the variables.

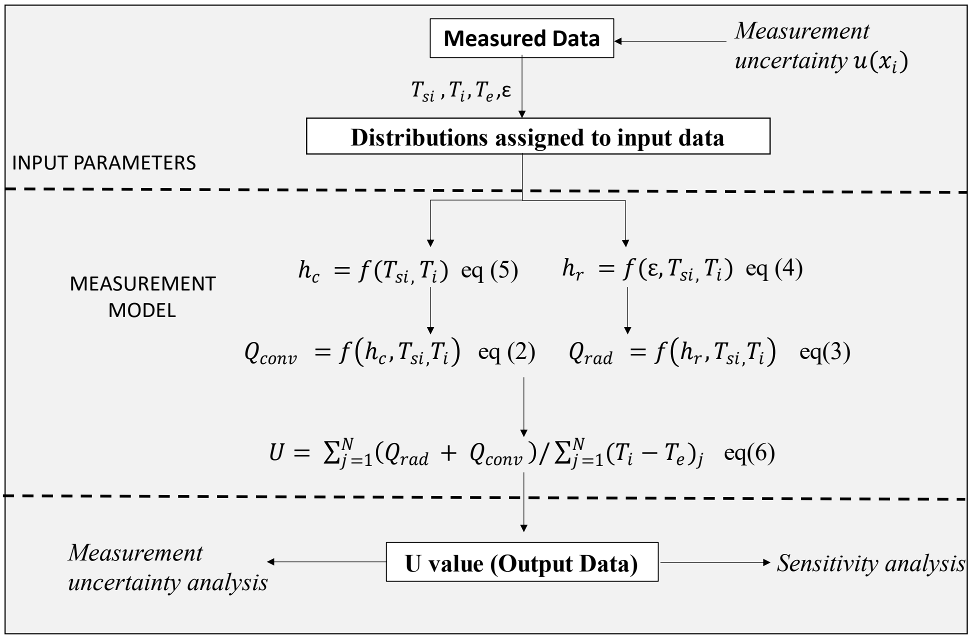

Figure 9 Model of Measurement of the thermal transmittance using IR sensor

The uncertainty propagation method [27] was used to evaluate the deviation of the U-value measured by means of Comfort Eye's IR system with respect to the value obtained with the HFM method, which was taken as a reference in this study. It is important to underline that the uncertainty values estimated in this analysis should not be considered as the absolute uncertainty of the tool but rather as a discrepancy with respect to the reference HFM, which, in addition, includes its own component of uncertainty. The variables involved were assumed to be statistically uncorrelated. MCM provides a generic method for numerically approximating the cumulative density function (*cdf*) of the output of a specific variable $y = f(x)$. MCM is based on the concept that any sample of x_i (input quantity) selected from a predetermined distribution can be employed. Consequently, by randomly sampling each input x_i, it is possible to estimate a potential output *y* outcome and its related uncertainty using the corresponding probability distribution function (*pdf*).

In the analysis presented, MCM consisted in the following steps:

1) the number of trials, N, was fixed to 10^6, which provides a 95% coverage interval, as described in the GUM supplement. The greater N, the higher the expected convergence of outcomes;
2) M vectors x_i, i = 1,…. M, in this case M = 4, were derived by randomly picking from the *pdfs* of each input quantity, i.e. [T_i, T_{si}, T_e, ε] for the IR model (Comfort Eye) and [T_i, T_e, q] for the HFM model, to obtain potential inputs to be correlated to x_i;
3) for each of the vectors obtained in point two, the analogous output *y* (U-value) was computed using both the models considered in this work, i.e. i) the HFM model, ii) the IR model with Comfort Eye using the h_c values calculated by ASHRAE and Wilkers. The dimension of the output was therefore M;
4) the representation G of the distribution functions of Y was generated starting from the set of M outputs of Y;

5) G was used to obtain the appropriate coverage region of Y;
6) the sensitivity coefficients $c_i\ (x_i)$ were calculated.

Tables 3, 4 and 5 show the standard uncertainty $u(x_i)$, the uncertainty of the output $u_i\ (y)$ and the sensitivity coefficients $c(x_i)$, which are the final output of the analysis.

Equation (9) was used to calculate the sensitivity coefficients $c(x_i)$:

$$c(x_i) = \frac{u_i\ (y)}{u(x_i)} \tag{9}$$

In accordance with the concept of maximum entropy, since the sole information on the quantity X was its range limit, a rectangular distribution was used for ε, with an upper limit b = 0.97 and a lower limit a = 0.93. Whereas, a Gaussian distribution was used for $T_{si,}T_i, T_e,$ since the best estimate x and associated standard uncertainty u(x) were the sole information on the quantity X. The uncertainty of T_e (Type T Thermocouple) was derived from the datasheet of the sensor, while the uncertainties of $T_i, T_{si,}$ were obtained from the analyses carried out in previous works [33][36]. The heat transfer coefficients h_c and h_r were not directly perturbed, since they were calculated from T_{si},T_i, ε, which are the input quantities considered for the implementation of the Monte Carlo simulation. MCM was applied to each of the three-time windows analysed (I, II, III) considering both the values of h_c defined by ASHRAE and Wilkers. In the Comfort Eye model, the generated distribution for ε is only taken into account in the equation 4, as the emissivity uncertainty has been evaluated in previous studies to calculate the measurement uncertainty o f the IR sensor of the Comfort Eye [33][36].Thus, the uncertainty of ε is already included in the uncertainty of the input parameter T_{si}. For clarity, the surface temperature values used by the Comfort Eye tool are retrieved automatically from a MySQL database (Figure 2) where the correction of the emissivity according to the equation 8 is already applied. The procedure used for Comfort Eye was also applied to the HFM reference method for each time window. In this case, the input variables were the heat flux measured by the HFP01 sensor with an uncertainty of 3% with k=2 [35] and the T_i and T_e temperatures measured by the Type T thermocouple with an uncertainty of ±0.5 °C. Also in this case, a Gaussian distribution was used for T_i ,T_e,q. This approach ensures an accurate and comprehensive analysis of the data, improving the robustness and reliability of the results. The results obtained from the computation performed are summarised in the Tables below.

In Table 3, the uncertainties for each variable are reported as standard deviations, along with their associated distributions for both Comfort Eye and HFM models. All distributions were generated with a mean equal to 0, and the sample from the distribution was added to the value used in the reference condition during the calculation.

Table 3 Input Variables with standard deviation and distribution for both, Comfort Eye and HFM Model.

Comfort Eye			**HFM**		
Input Variable	$u(x_i)$	Distribution	Input Variable	$u(x_i)$	Distribution
$\boldsymbol{T_{si}}$	± 1K	Gaussian	Heat Flux (q)	± 3%	Gaussian
$\boldsymbol{T_i}$	± 0.5 K	Gaussian	$\boldsymbol{T_i}$	± 0.5 K	Gaussian
$\boldsymbol{T_e}$	± 0.5 K	Gaussian	$\boldsymbol{T_e}$	± 0.5 K	Gaussian
ε	± 0.014	Rectangular	/	/	/

Table 4reports the values obtained with MCM for the measurements performed using Comfort Eye with the value of h_c defined by ASHRAE in the time windows I, II, and III (Figure 5,Figure 6Figure 7). The values of $u_i(y)$ are expressed in $[\frac{W}{m^2K}]$ while those of $c(x_i)$ are expressed in $[\frac{W}{m^2K^2}]$ for T_{si}, T_i, T_e and in $\left[\frac{W}{m^2K}\right] for\ \varepsilon$.

Table 4 Output of the Monte Carlo Analysis – Comfort Eye (ASHRAE)

$\boldsymbol{h_c}$ **ASHRAE**	**Window I**		**Window II**		**Window III**	
Input Variables	$u_i(y)$	$c(x_i)$	$u_i(y)$	$c(x_i)$	$u_i(y)$	$c(x_i)$
$\boldsymbol{T_{si}}$	0.01	0.02	0.01	0.02	0.01	0.02
$\boldsymbol{T_i}$	0.008	0.02	0.008	0.02	0.007	0.016
$\boldsymbol{T_e}$	0.001	0.003	0.001	0.003	0.001	0.002
ε	0.002	0.01	0.002	0.012	0.001	0.01

The Monte Carlo simulation provided an expanded uncertainty of ± 0.04, ±0.044 and ±0.04 W/m^{2}K with k=2 on the U-value measurements in time windows I, II III, respectively. Figure 10 shows the representation of the distribution functions of the U-value derived from the Monte Carlo simulation when all the inputs are perturbed with their measurement uncertainty. The 95% confidence interval is respectively of 0.08, 0.088 and 0.08 W/m^{2}K for the three time windows considered.

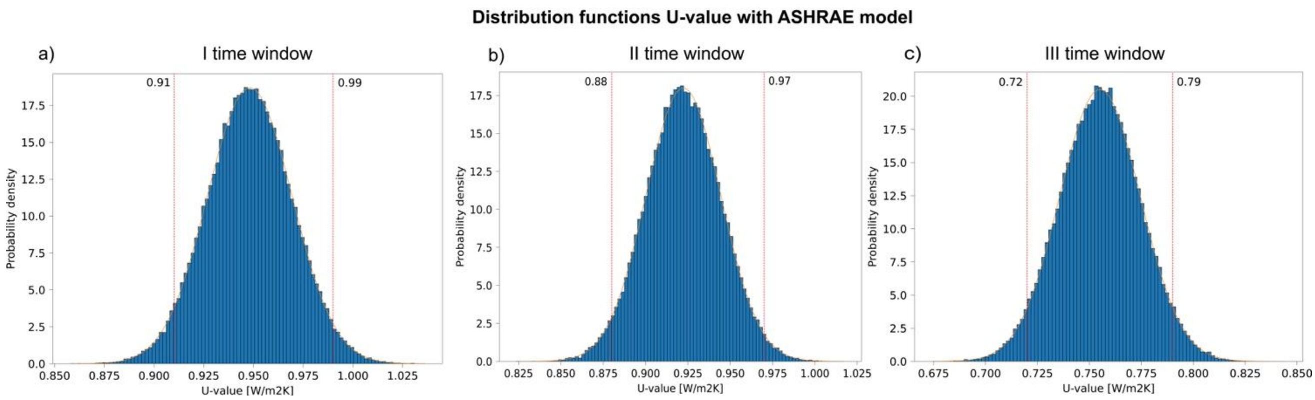

Figure 10 Representation of the distribution function for the U-value measured with the IR sensor with ASHRAE model

Table 5 reports the values obtained with MCM for the measurements performed using Comfort Eye with the value of h_c defined by Wilkers in time windows I, II, and III, respectively. The values of $u_i(y)$ are expressed in $[\frac{W}{m^2K}]$ while those of $c(x_i)$ are expressed in $[\frac{W}{m^2K^2}]$ for T_{si}, T_i, T_e and in $\left[\frac{W}{m^2K}\right] for\ \varepsilon.$

Table 5 Output of the Monte Carlo Analysis- Comfort Eye (Wilkers)

h_c **Wilkers**	**Window I**		**Window II**		**Window III**	
Input Variables	$u_i(y)$	$c(x_i)$	$u_i(y)$	$c(x_i)$	$u_i(y)$	$c(x_i)$
T_{si}	0.02	0.024	0.02	0.024	0.02	0.021
T_i	0.01	0.021	0.01	0.021	0.01	0.02
T_e	0.001	0.003	0.001	0.003	0.001	0.002
ε	0.002	0.012	0.002	0.012	0.001	0.01

The Monte Carlo simulation for Comfort Eye provided an expanded uncertainty of ± 0.05, W/m^{2}K with k=2 on the U-value measurements in time windows I, II III.Figure 11 shows the representation of the distribution functions of the U-value derived from the Monte Carlo simulation when all the inputs are perturbed with their measurement uncertainty. The 95% confidence interval is equal to 0.1 W/m^{2}K for the three time windows considered.

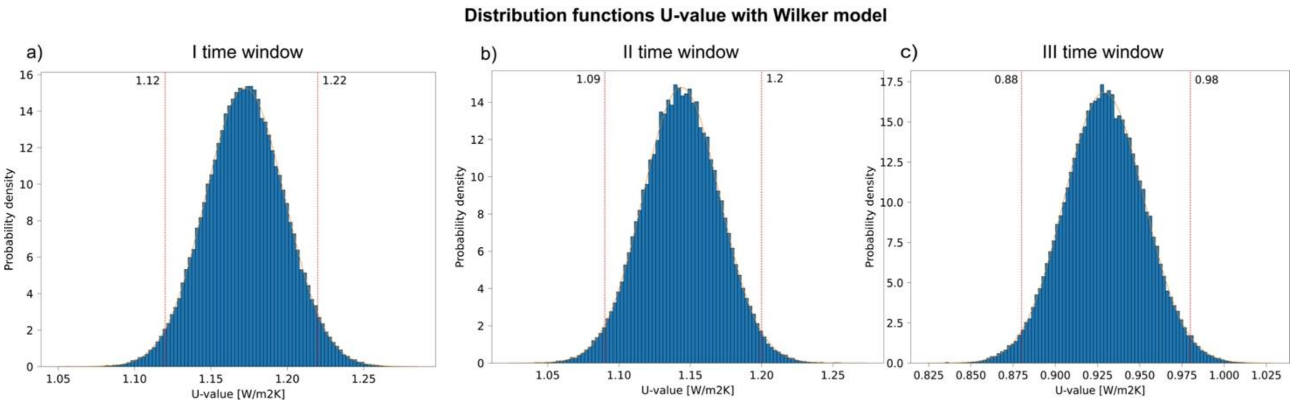

Figure 11 Representation of the distribution function for the U-value measured with the IR sensor with Wilkers model

Table 6 reports the values obtained with MCM for the measurements performed with the HFM for time windows I, II, and III. The values of $\mathrm{u_i(y)}$ are expressed in $[\frac{\mathrm{W}}{\mathrm{m^2K}}]$ while those of $\mathrm{c(x_i)}$ are expressed in $[\frac{\mathrm{W}}{\mathrm{m^2K^2}}]$ for T_i, T_e and in $\left[\frac{1}{K}\right] for\ q.$

Table 6 Output of the Monte Carlo Analysis- HFM

HFM	**Window I**		**Window II**		**Window III**	
Input Variables	$u_i(y)$	$c(x_i)$	$u_i(y)$	$c(x_i)$	$u_i(y)$	$c(x_i)$
Heat Flux (*q*)	0.001	0.003	0.001	0.003	0.001	0.002

T_i	0.001	0.002	0.001	0.002	0.001	0.002
T_e	0.001	0.002	0.001	0.002	0.001	0.002

The Monte Carlo simulation for the HFM method provided an expanded uncertainty of ±0.004 W/m^{2}K with k=2 on the U-value measurements in time windows I, II, III, respectively. Figure 12 shows the representation of the distribution functions of the U-value derived from the Monte Carlo simulation when all the inputs are perturbed with their measurement uncertainty. The 95% confidence interval is of 0.008 W/m^{2}K for all three the time windows.

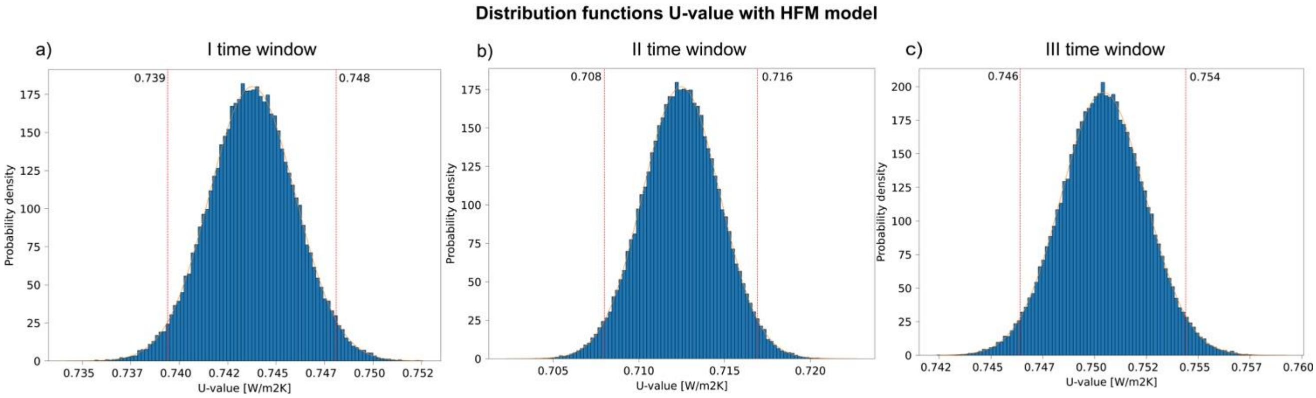

Figure 12 Representation of the distribution function for the U-value measured with the HFM model

To understand the actual applicability of the approach proposed under real environmental conditions, an additional variance-based sensitivity analysis was performed to test the hypothesis of uncorrelated inputs for the Comfort Eye approach. The sensitivity analysis was carried out by considering the influence of the input parameters.

The general procedure consists in calculating the first order sensitivity indexes (S_i) according to the method described in [38], which is a variance-based method:

$$S_i = \frac{V_{x_i}}{V_{tot}} \tag{9}$$

where V_{xi} is the output variance when considering as input only the random distribution of the parameter x_i while keeping the other parameters constant, and V_{tot} is the total variance of the output due to the perturbation of the model when considering as input the random distribution of all the inputs. Thus, each index can be represented as a percentage of the total variance of the output. As a result, the sum of all the S_i is equal to 98%, which is near to unity (100%). This demonstrates that only minor correlations are present, and inputs can be considered as being uncorrelated with a negligible impact on the uncertainty analysis.

6.2 Discussion of the results

The uncertainty of the method proposed was evaluated through Monte Carlo simulations. The following figure shows the results in terms of mean and standard deviations of the uncertainty analysis for the IR model with the values of h_c defined by Wilkers and ASHRAE and for the HFM reference method in the three-time windows**.**

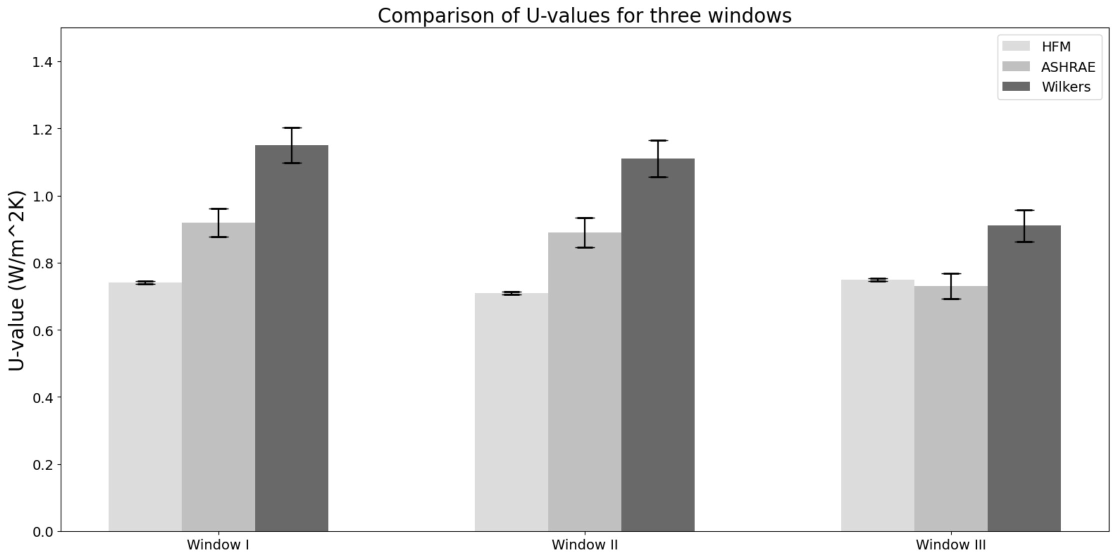

Figure 13 Mean and Standard deviations with k= 2 for the IR model with the values of h_c defined by ASHRAE and Wilkers and for the HFM model in the three time windows

6.3 The figure (Figure 13) presented in this section clearly illustrates how the choice of the h_c coefficient can significantly impact U-value measurements. Moreover, the results indicate that the measurement accuracy is highly dependent on operating conditions. Concerning the impact of the input uncertainty, the most accurate result for the IR model (Comfort Eye) was obtained in time window III using the value of $h_c$defined by ASHRAE. In this time window, the mean and standard deviation values for the HFM, ASHRAE, and Wilkers methods were respectively 0.75 ± 0.004, 0.73 ± 0.04, and 0.91 ± 0.05 $\mathrm{W/m^2K}$ with k=2. It is worth noting that in time window III the temperature difference was greater than 10°C for more than 50% of the time, as shown in Figures 5, 6, and 7. Moreover, a systematic deviation on the final U-value between the HFM and IR model was found in all the time windows. In particular, such deviation was higher for window I and II, when the conditions required by the standard are not completely satisfied. Therefore, such deviation should be corrected when using the IR model. In this particular case, considering the ASHRAE model, the correction factors are -0.18, -0.18 and +0.02 W/m^{2}K for the three time windows, respectively. These findings suggest that the selection of an appropriate time window for the measurements is crucial and should, therefore, be taken into careful consideration. Overall, the methodology proposed can serve as a useful tool for U-value estimation without the need for extra measuring tools. However, further research is necessary to validate the methodology under different operating conditions and for different building types.**Guideline for application**

Considering the results reported and the functionalities of Comfort Eye, the system not only provides an analysis of indoor environmental conditions, particularly regarding thermal comfort and air quality, but it also allows the analysis of the thermal performance of a wall. The calculation of the heat transfer coefficient (U-value) is more accurate with a temperature difference between interior and exterior environments greater than 10 °C for a period exceeding 50% of the time. Based on this premise, Comfort Eye allows real time monitoring for long periods and the storage of the data collected in the MySQL database, therefore it makes it possible to select among the data collected those that meet the standard requirements. When using the Comfort Eye system, should it not be possible to install a sensor to measure external temperature, the necessary data can be extracted from an external weather station via an API service.

Once the data are selected, the heat transfer coefficient model can be applied to provide an analysis of the thermal performance of the wall (Figure 14). As the system can be installed for long periods, this process can be repeated multiple times to evaluate changes in the thermal performance over time.

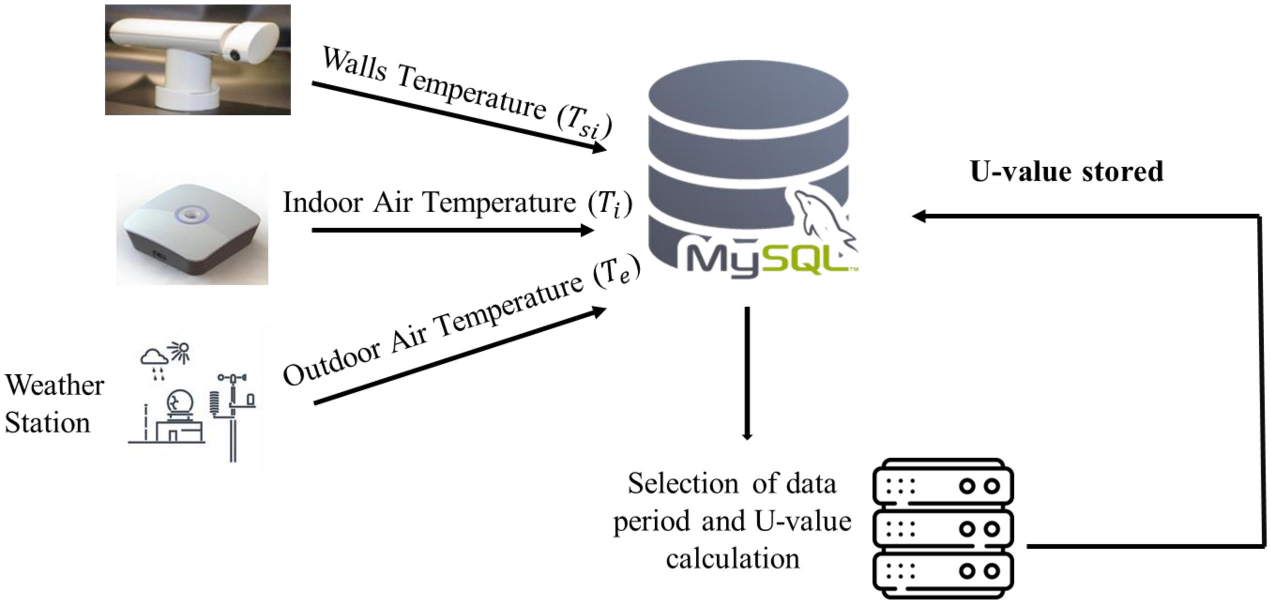

Figure 14 Workflow for U-value calculation using Comfort Eye and weather data. The model makes it possible to select the time window with a temperature difference between the interior and exterior environments greater than 10 °C

7. Conclusions

A method for U-value in-situ experimental determination based on the measurement of indoor surface temperature using an IoT, non-contact, full-field IR sensor was proposed. Comfort Eye, a system for the evaluation of IEQ which is equipped with an IR sensor, was adopted to measure the inside surface temperature of a façade wall. The method was validated through a test in a real environment and the measurements were taken according to ISO 9869-1 and ISO 9869-2 procedures.

This paper shows that the method proposed for U-value calculation under realistic environmental conditions is reliable. In the case presented, the outcomes demonstrated that the best result is obtained with the heat transfer coefficient h_c reported by ASHRAE and a ΔT between indoor and outdoor air temperature greater than 10 °C for at least 50 % of the time, which is in line with the requirements of ISO 9869-2. Different time windows were analysed to demonstrate the repeatability of the methodology applied. When monitoring in real environmental conditions, however, this requirement could be a limitation. The Comfort Eye sensor makes it possible to overcome this limitation by performing long-term monitoring and selecting only time-windows with a ΔT greater than 10°C.

The paper also illustrated the application of MCM to analyse the measurement uncertainty of thermal transmittance using the IR system (Comfort Eye). The aim is to identify the measurement uncertainty of the U-value by applying the GUM guidelines and the Monte Carlo method to define the impact of the measurement uncertainty of the sensors used to monitor the data necessary to calculate the U-value. The results obtained indicate that the measurement accuracy is highly dependent on operating conditions. The most accurate result for the IR model was obtained using the value of h_c defined by ASHRAE in time window III. In this time window, the mean and standard deviation values for the HFM, ASHRAE, and Wilkers methods were respectively 0.75 ± 0.004, 0.73 ± 0.04, and 0.91 ± 0.05 (W/m^2K) with k=2. It is worth noting that in time window III the temperature difference was greater than 10°C for more than 50% of the time, as shown in Figures 5, 6, and 7. These findings suggest that the choice of an appropriate time window for the measurements is crucial and should, therefore, be taken into careful consideration. The results showed that different environmental quantities produce different uncertainties of the U-value. T_{si} contributed the most to this uncertainty, since U (T_{si}) = ±1 °C. The variance-based sensitivity analysis demonstrates that the input parameters can be considered as being uncorrelated.

In conclusion, the methodology provides an innovative solution for the measurement of the indoor surface temperature of a wall in a built environment, making it possible to determine the U-value. It is important to underline that the uncertainty values estimated in this analysis should not be considered as the absolute uncertainty of the tool but rather as the discrepancy with respect to the reference HFM model, which, in addition, includes its own component of uncertainty. The final result is that the IR system presents a confidence interval of the measured U-value that is one order of magnitude higher than the one achieved with the HFM system.

Thanks to its ability to perform real-time and continuous monitoring and for long periods, Comfort Eye has the capability to identify changes in surface heat over time. Therefore, the thermal dynamic behaviour of a whole wall can be available in real-time. Even under real environmental conditions, the calculation of thermal transmittance using the IR method showed good accuracy. Thermal bridges can affect the accuracy of U-value measurements and for this reason further analyses will be considered in future investigations in order to understand how much the selection of the ROI could affect the thermal transmittance measurements.

Data availability

The data that support the findings of this study are available upon request from the authors.

References

[1] A. Tahmassebia, A. H. Gandomib, "Building energy consumption forecast using multi-objective genetic", Measurement 118 (2018) 164–171.

[2] I. Jabłon´ ski "Integrated living environment: Measurements in modern energy efficient smart building with implemented the functionality of telemedicine" Measurement 101 (2017) 211–235.

[3] Principi, P., Roberto, F., Carbonari, A., & Lemma, M. (2016). Evaluation of energy conservation opportunities through Energy Performance Contracting: A case study in Italy. *Energy and Buildings*, *128*, 886-899.

[4] T. Kurczveil, P. Diekhake, J. Liu, E. Schnieder, "Consumer load measurement in automated buildings", Measurement 51 (2014) 441–450.

[5] M. Nilashi, M. Dalvi-Esfahani, O. Ibrahim, K. Bagherifard, A. Mardani, N. Zakuan "A soft computing method for the prediction of energy performance of residential buildings", Measurement 109 (2017) 268–280.

[6] Guo, M., Zhou, M., Wei, S., Peng, J., Wang, Q., Wang, L., Cheng, D., & Yu, W. (2021). Particle removal effectiveness of portable air purifiers in aged-care centers and the impact on the health of older people. Energy and Buildings, 250, 111250.

[7] Park H, Martaj N, Ruellan M, Bennacer R, Monmasson E. Modeling of a Building System and its Parameter Identification [Internet]. Vol. 8, Journal of Electrical Engineering and Technology. The Korean Institute of Electrical Engineers; 2013. p. 975–83

[8] EN ISO 6949, Building components and building elements – Thermal resistance and Thermal transmittance – Calculation method, 2007.

[9] ISO 8990, Thermal insulation - Determination of steady-state thermal transmission properties - Calibrated and and guarded hot box, 1994

[10] ISO 9869-1, Thermal insulation – Building elements – In-situ measurement of thermal resistance and Thermal transmittance – Part 1: Heat flow meter method, 2014.

[11] X. Meng, T. Luo, Y. Gao, L. Zhang, Q. Shen and E. Long, "A new simple method to measure wall

thermal transmittance in situ and its adaptability analysis", *Applied Thermal Engineering*, vol. 122, p. 747–757, 2017.

[12] K. Gała̜zka, S. Populoh, W. Xie, J. Hulliger, A. Weidenkaff "Radiative heat losses in thermal conductivity measurements: a correction for linear temperature gradients", Measurement 90 (2016) 187–191.

[13] A. Rasooli, L. Itard, "In-situ characterization of walls' thermal resistance: An extension to the ISO 9869 standard method" Energy & Buildings 179 (2018) 374–383

[14] M. Cucumo, A. De Rosa, V. Ferraro, D. Kaliakatsos and V. Marinelli, "A method for the experimental evaluation in situ of the wall conductance," *Energy and Buildings*, vol. 38, pp. 238-244, 2006.

[15] R. Albatici and A. M. Tonelli, "Infrared thermovision technique for the assessment of thermal transmittance value of opaque building elements on site", *Energy and Buildings*, vol. 42, pp. 2177-2183, 2010.

[16] R. Albatici, A. M. Tonelli and M. Chiogna, "A comprehensive experimental approach for the validation of quantitative infrared thermography in the evaluation of building thermal transmittance", *Applied Energy*, vol. 141, pp. 218-228, 2015.

[17] A. G. Mainini, T. Poli, R. Paolini, M. Zinzi and L. Vercesi, "Transparent multilayer ETFE panels for building envelope: thermal transmittance evaluation and assessment of optical and solar performance decay due to soiling", in SHC 2013, *International Conference on Solar Heating and Cooling for Buildings and Industry*, Freiburg, Germany, 2013.

[18] Ohlsson, K.E.A. and T. Olofsson, Quantitative infrared thermography imaging of the density of heat flow rate through a building element surface. Applied Energy, 2014. 134: p. 499-505.

[19] Fokaides, P.A. and S.A. Kalogirou, Application of infrared thermography for the determination of the overall heat transfer coefficient (UValue) in building envelopes. *Applied Energy*, 2011. 88(12): p. 4358-4365.

[20] I. Danielski and M. Fröling, "Diagnosis of buildings' thermal performance - a quantitative method using thermography under non-steady state heat flow", in *7th International Conference on Sustainability in Energy and Buildings*, Lisbon, Portugal, 2015.

[21] M. Teni, H. Krstić, P. Kosiński, Review and comparison of current experimental approaches for in-situ measurements of building walls thermal transmittance, Energy and Buildings, Volume 203, 2019.

[22] D. B-Huertas, J.Moyano, D. Marín, R. F.Contreras, Review of in situ methods for assessing the thermal transmittance of walls, Renewable and Sustainable Energy Reviews, Volume 102, 2019,Pages 356-37

[23] ISO 9869-2, Thermal insulation- Building elements In-situ measurement of thermal resistance and thermal transmittance – Infrared method for frame structure dwelling, 2018.

[24] S.Serroni, M. Arnesano, G. Pandarese,M.Martarelli, G.M. Revel, IoT infrared sensor for continuos monitoring of building envelope thermal perfomances, Splitech 2021

[25] S.Serroni, M. Arnesano, M.Martarelli, G.M. Revel, Application of an IoT infrared sensor for thermal

transmittance measurment in building renovation, Splitech 2022

[26] BIMSPEED Project : https://www.bim-speed.eu/en

[27] GUM - JCGM 101, Evaluation of measurement data - Supplement 1 to the “Guide to the expression of uncertainty in measurement” — Propagation of distributions using a Monte Carlo method, 2008

[28] Fokaides, P. A., & Kalogirou, S. A. (2011). Application of infrared thermography for the determination of the overall heat transfer coefficient (U-Value) in building envelopes. *Applied Energy*, *88*(12), 4358-4365.

[29] Usamentiaga R, Venegas P, Guerediaga J, Vega L, Molleda J, Bulnes FG. Infrared thermography for temperature measurement and non-destructive testing. Sensors (Basel). 2014 Jul 10;14(7):12305-48.

[30] Acikgoz, O.; Kincay, O. Experimental and numerical investigation of the correlation between radiative and convective heat-transfer coefficients at the cooled wall of a real-sized room. Energy Build. 2015, 108, 257–266.

[31] Antunovi´c, B.; Stankovi´c, M.; Jankovi´c, A.; Gaji´c, D.; Todorovi´c, D. Measurement of thermal transmittance in the Rectorate building of the University of Banja Luka. In Proceedings of the International Scientific Conference Contemporary Theory and Practice in Civil Engineering, Banja Luka, Bosnia and Herzegovina, 26–27 April 2012; pp. 37–46

[32] M. Gaši , B. Milovanovi´, S. Gumbarevi, "Comparison of Infrared Thermography and Heat Flux Method for Dynamic Thermal Transmittance Determination, Buildings 2019, 9, 132;

[33] G.M.Revel, M. Arnesano, F.Pietroni, “Development and validation of a low-cost infrared measurement system for real-time monitoring of indoor thermal comfort”, Measurement Science and Technology 25 (2014) 085101 (10pp)

[34] S.Serroni, M.Arnesano, L.Violini, G.M.Revel, A IoT measurment solution for continuous indoor environmental quality monitoring for buildings renovation., Acta Imeko, Vol. 10 2021

[35] https://www.hukseflux.com/products/heat-flux-sensors/heat-flux-sensors/hfp01-heat-flux-sensor

[36] Lorenzo Zampetti, Development of a low-cost system for thermal comfort measurement and control. PhD Thesis, 2017

[37] N.Morresi, S.Casaccia,M.Arnesano, G.M.Revel, Impact of the measurement uncertainty on the monitoring of thermal comfort through AI predictive algorithms., Acta Imeko, Vol. 10 2021

[38] Saltelli, A., Ratto, M., Andres, T., Campolongo, F., Cariboni, J., Gatelli, D., Saisana, M. and Tarantola, S. (2007). Variance-Based Methods. In Global Sensitivity Analysis. The Primer (eds A. Saltelli, M. Ratto, T. Andres, F. Campolongo, J. Cariboni, D. Gatelli, M. Saisana and S. Tarantola)